Non-destructive identification of chemical composition for iron compounds using chemical environmental effect on muon capture process

Kazuhiko Ninomiya[1,2], Meito Kajino[2], Akihiro Nambu[2], Makoto Inagaki[2,3], Takuto Kudo[2], Akira Sato[2], Kentaro Terada[2], Atsushi Shinohara[2,4], Dai Tomono[5], Yoshitaka Kawashima[5], Yoichi Sakai[6], Tsutomu Takayama[6]

[1]*Insititute for Radiation Sciences, Osaka University, Toyonaka, Osaka 560-0043, Japan*

[2]*Graduate School of Science, Osaka University, Toyonaka, Osaka 560-0043, Japan*

[3]*Institute for Integrated Radiation and Nuclear Science, Kyoto University, Kumatori, Sennan, Osaka 590-0494, Japan*

[4]*Osaka Aoyama University, Minoh, Osaka 562-8580, Japan*

[5]*Research Center for Nuclear Physics, Osaka University, Ibaraki, Osaka 567-0047, Japan*

[6]*Department of Chemistry, Daido University, Takiharu-cho, Nagoya, Aichi 457-8530, Japan*

In recent years, elemental analysis method using muon beam (MIXE: Muon Induced X-ray Emission) has been developed and applied for various research fields [1-9]. This method identifies elements by measuring characteristic “muonic” X-rays emitted from a material after muon irradiation. Since the mass of a muon is approximately 200 times greater than that of an electron, the energies of muonic X-rays are also approximately 200 times higher than those of characteristic electronic X-rays. Even for light elements such as lithium and carbon, the energies of the X-rays are so high that they are hardly absorbed in the sample itself. Furthermore, the muon stopping depth in a material can be controlled by selecting the incident muon beam momentum; that is, the analysis depth can be selected. Using these properties, MIXE can identify elements inside a material non-destructively and regioselectively.

Although the radius of the muon atomic orbit is much smaller than that of the electrons, chemical environmental effects are known in muonic atom formation. For example, in CO and CO_2, the muon capture probabilities of carbon and oxygen atoms are different even if are corrected for the number of atoms in these molecules. A carbon atom in CO is more likely to capture muons than the carbon atom in CO_2 by approximately 40% [10]. Simultaneously, the initial atomic orbit of the captured muon also changes depending on the chemical state. As a results, muonic X-ray intensity patterns, for example, emission probabilities of 2p-1s and 3p-1s X-rays varies by chemical state.

By utilizing such a chemical effect on the muon capture process, further developments of MIXE, the identification of not only the element but also the chemical state of each element, becomes possible. In this study, we demonstrated non-destructive chemical state analysis of iron oxides by muonic X-ray measurements [11].

The muon experiment was conducted as an E529 experiment. The experimental system was

constructed at the MuSIC-M1 beamline in RCNP [12] with the same experimental setup described elsewhere [11]. The muonic X-rays emitted after the muon stopped in the sample were measured using two high-purity germanium semiconductor detectors (Mirion Technology Canberra, BE3830 and GC6020). The timing of the muon stop in the sample was identified using a coincidence signal from a pair of plastic scintillation counters placed in front of the sample. The detection efficiency for each muonic X-ray was estimated by Monte Carlo calculations using the EGS-5 code (Electron Gamma Shower 5 [13]) based on the actual measurement data of a standard radioactive source.

In this study, iron sand was selected as the target for non-destructive chemical state analysis. Iron sand is generally a mixture of γ-Fe_2O_3 and Fe_3O_4, and the content of γ-Fe_2O_3 for the iron sand sample was determined as 25.6(7)% by Mössbauer analysis. We conducted muon irradiation for the iron sand powders, γ-Fe_2O_3 and Fe_3O_4 with the muon incident momentum of 52.5 MeV/c. The typical muon intensity measured using plastic scintillation counters was 500 muons/s.

Figure 1 shows the muonic X-ray spectrum obtained from the muon irradiation of the iron sand sample. X-ray peaks of the 2p-1s muon transitions in oxygen and iron atoms were observed at 133 keV and 1260 keV, respectively [14, 15]. In addition to these peaks, relatively minor muonic X-rays such as 3p-1s were also identified. Since some muonic oxygen X-ray peaks was overlapped by the signals from background, the background contributions were subtracted [11].

The muonic X-ray intensity pattern of iron for iron sand sample was reproduced by the mixture of these for γ-Fe_2O_3, and Fe_3O_4 samples [16]. Figure 2 shows the experimental muonic X-ray intensity pattern for the iron sand and estimated one by optimizing mixing ratio of γ-Fe_2O_3 and Fe_3O_4. The optimum contents of γ-Fe_2O_3 in the iron sand was estimated to be 25%; this value was in good agreement with the mixing ratio obtained by the Mössbauer analysis (25.6%). From these results, we succeeded in non-destructively determining the composition of iron sand from the intensity ratios of muonic X-rays.

We also estimated contents of γ-Fe_2O_3 in the iron sand in view point of muon capture ratio. The muon capture ratios for iron to oxygen atoms in γ-Fe_2O_3 and Fe_3O_4 were R(Fe/O)=1.58±0.01 and 2.08±0.02, respectively [16]. The muon capture ratio for the iron sand sample in this work was R(Fe/O)=1.90±0.10. This value exists between those of γ-Fe_2O_3 and Fe_3O_4 and is consistent with the fact that iron sand is composed of γ-Fe_2O_3 and Fe_3O_4. The γ-Fe_2O_3 component in the iron sand was determined to be 19%, which is consistent with the results of the Mössbauer analysis (25.6%) and muonic X-ray intensity ratio (25%).

In this study, the chemical composition analysis by muonic X-ray measurement was firstly demonstrated. In principle, such chemical environmental effects on muon capture appear not only in iron but in any elements. It is possible to determine the chemical state deep inside a material non-destructively; for example, the oxidation state of a metal can be known for valuable samples such as archaeological artifacts.

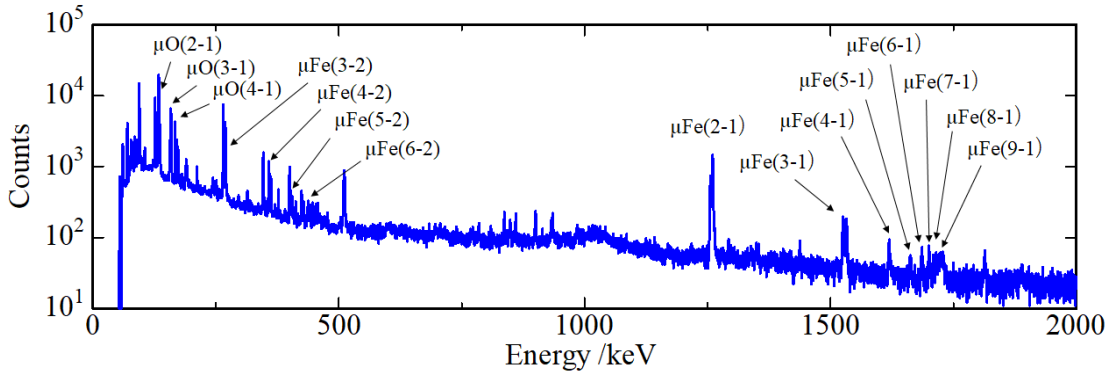

Figure 1: Muonic X-ray spectrum for the iron sand sample. The numbers in parentheses indicate the change in the principal quantum numbers of the muon via muonic transition.

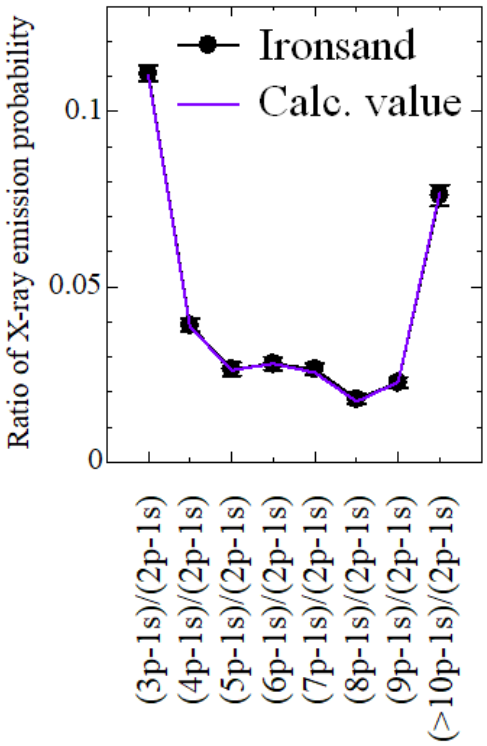

Figure 2: Experimental muonic X-ray emission pattern for the iron sand sample. The calculated muonic X-ray pattern was obtained from the mixture of 25 % of γ-Fe_2O_3 and 75 % of Fe_3O_4.

References

[1] K. Ninomiya *et al*., Bull. Chem. Soc. Jpn. **85**, 228 (2012).

[2] K. Terada *et al*., Sci. Rep. **4**, 5072 (2014).

[3] K. Ninomiya *et al*., Anal. Chem. **87**, 4597 (2015).

[4] K. Terada *et al*., Sci. Rep. **7**, 15478 (2017).

[5] B. V. Hampshire *et al*., Heritage **2**, 400 (2019).

[6] I. Umegaki *et al*., Anal. Chem. **92**, 8194 (2020).

[7] K. Shimada-Takaura *et al*., J. Nat. Med. **75**, 532 (2021).

[8] T. Nakamura *et al*., Science. **379**, eabn8671 (2022).

[9] S. Biswas *et al*., Heritage Sci. **11**, 43 (2023).

[10] G. Yoshida *et al*., J. Radioanal. Nucl. Chem. **320**, 283 (2019).

[11] K. Ninomiya *et al*., Bull. Chem. Soc. Jpn. **95**, 1769 (2022).

[12] S. Cook *et al*., Phys. Rev. Accel. Beams **20**, 030101 (2017).

[13] H. Hirayama *et al*., THE EGS5 CODE SYSTEM, SLAC-R-730 and KEK Report 2005-8 EGS5 (2005).

[14] G. Fricke *et al*., Atom. Data Nucl. Data Tab. **60**, 177 (1995).

[15] F. J. Hartmann *et al*., Phys Rev Lett. **37**, 331 (1976).

[16] K. Ninomiya *et al*., J. Radioanal. Nucl. Chem. **324**, 403 (2020).